Thermodynamic bounds for diffusion in nonequilibrium systems with multiple timescales

A. Plati,[1,2,3] A. Puglisi,[1,2,4] and A. Sarracino[5,2]

[1]*Department of Physics, University of Rome Sapienza, Piazzale Aldo Moro 2, 00185, Rome, Italy*
[2]*Institute for Complex Systems–CNR, Piazzale Aldo Moro 2, 00185, Rome, Italy*
[3]*Université Paris-Saclay, CNRS, Laboratoire de Physique des Solides, 91405 Orsay, France*
[4]*INFN, University of Rome Tor Vergata, Via della Ricerca Scientifica 1, 00133, Rome, Italy*
[5]*Department of Engineering, University of Campania "Luigi Vanvitelli," 81031 Aversa (CE), Italy*

(Received 11 July 2022; revised 10 January 2023; accepted 21 March 2023; published 28 April 2023)

We derive a thermodynamic uncertainty relation bounding the mean squared displacement of a Gaussian process with memory, driven out of equilibrium by unbalanced thermal baths and/or by external forces. Our bound is tighter with respect to previous results and also holds at finite time. We apply our findings to experimental and numerical data for a vibrofluidized granular medium, characterized by regimes of anomalous diffusion. In some cases our relation can distinguish between equilibrium and nonequilibrium behavior, a nontrivial inference task, particularly for Gaussian processes.

DOI: 10.1103/PhysRevE.107.044132

I. INTRODUCTION

The relation between dynamical properties of a system and its thermodynamics plays a central role in modern nonequilibrium statistical physics. In systems composed by many interacting particles, it is common to observe different phenomena occurring at different timescales, the paradigmatic example being the several regimes of structural relaxation in undercooled liquids [1]. This complex dynamics usually gives place to a mean squared displacement (MSD) of some fluctuating observable which shows several nondiffusive regimes. For instance, the diffusion of particles in liquids often displays transient subdiffusive or flat MSD corresponding to cage effects. Interestingly, these regimes are also observed in liquidlike systems realized by replacing molecules with macroscopic spheres, in the context of dense vibrofluidized granular materials, both in simulations and in experiments [2–5]. Additionally, these systems can display novel phenomena such as a superdiffusive transient regime after the cage stage and before the final asymptotic standard diffusion [6]. While the molecular liquid case is typically at thermal equilibrium (even if under sudden quench the relaxation time may diverge and shift the system into nonequilibrium), a vibrated granular medium is intrinsically out of equilibrium, even if stationary, because of the presence of several energy flows from and into the system (friction, inelastic collisions, external energy pumping, etc.). In principle, however, diffusion properties are not evidently related to the status of equilibrium or nonequilibrium [7]. It is therefore important to explore the existence of physical constraints that could restrict the possible behaviors of the MSD and relate certain observations to the thermodynamic status of the system [8].

Recently, an important step in building a bridge between anomalous dynamical regimes and thermodynamic properties has been done exploiting the thermodynamic uncertainty relations (TURs) [9,10]. These relations, valid for quite a large class of stochastic processes, also demonstrated through several different routes [11–14], typically take the form

$$\frac{\langle \Delta\theta(t)^2 \rangle}{\langle \theta(t) \rangle^2} \geqslant \frac{2}{\langle S(t) \rangle}, \tag{1}$$

where $\Delta\theta(t) = \theta(t) - \langle \theta(t) \rangle$, and $\theta(t) = \int_0^t dt'\, \omega(t')$ is an integrated current over a time t, while $S(t)$ is the entropy produced by the system in the same time interval. Here and throughout the paper we fix $k_b = 1$. Identifying $\theta(t)$ as the displacement of a particle with velocity $\omega(t)$ and multiplying both sides of (1) for $\langle \theta(t) \rangle^2$, one obtains a straightforward application to the MSD, which has been applied to the case of overdamped systems with *two* dynamical regimes, one being anomalous and one being standard [15]. In particular, it has been shown that the TUR implies a minimum (or maximum) time of validity for the super- (or sub-) diffusion.

The application of this kind of result to nonequilibrium systems with multiple characteristic timescales requires a more general and effective bound, which is the purpose of the present paper. Here we show how to extend TURs for underdamped dynamics to the case of systems with multiple timescales and multiple baths, such as active liquids and vibrofluidized granular media. We obtain a general formula to bound the MSD in time, with the interesting and unexpected result that only a part of the entropy production enters the bound, making it tighter than that one would get using the whole entropy production. We present analytical results within the framework of Markovian continuous linear systems that can emerge from the Markovianization of systems with memory, representing, therefore, a very general tool for the study of coarse-grained variables in presence of hydrodynamic backflow [16,17] and in out-of-equilibrium many-body systems [18–20], including driven macroscopic dissipative systems such as granular materials [21] and active matter [22]. We recall that general thermodynamic bounds for underdamped dynamics still represent an open problem [12,23–25], while a TUR for non-Markovian system has been previously

derived for a very general class of memory kernels but always assuming thermal equilibrium with a single thermostat [26].

Our results are successfully applied to numerical and experimental data coming from two different systems of interacting particles where an intruder is immersed in a vibrated granular fluid [4,27]. Remarkably, our approach also shows that, in the zero driving limit, we obtain a TUR for the spontaneous diffusion that in fact can be tested with systems in the absence of an external bias, allowing one to distinguish between equilibrium and nonequilibrium behavior.

II. THE MODEL

We consider a set of $n+1$ coupled dynamical variables, each in contact with a different thermal bath. The first variable represents the main observable, possibly subject to a constant external force, while the other n variables are auxiliary variables, representing memory terms. This kind of model can describe the underdamped dynamics of a tracer in a fluid when a separation of timescales allows one to obtain an effective generalized Langevin equation (GLE) for the slow variable [28], or systems with feedback control [29–32]. Defining the vectors $\boldsymbol{X} = \{\omega, \Omega_1, \dots, \Omega_n\}$, $\boldsymbol{\xi} = \{\xi_0, \xi_1, \dots, \xi_n\}$, and $\boldsymbol{F} = \{F_{\rm ext}, 0, \dots, 0\}$, the dynamics is described by the coupled equations:

$$\dot{\boldsymbol{X}} = \hat{A}\boldsymbol{X} + \hat{B}\boldsymbol{\xi} + \boldsymbol{F}, \tag{2}$$

where ξ_i are uncorrelated white noises with zero mean and unit variance, while the two matrices $\hat{A}$ and $\hat{B}$ are given by

$$\hat{A} = \begin{pmatrix} -1/\tau & 1/b_1 & \dots & 1/b_n \\ -a_1 b_1 & -1/\tau_1 & 0 & 0 \\ \vdots & 0 & \ddots & 0 \\ -a_n b_n & 0 & 0 & -1/\tau_n \end{pmatrix}, \tag{3}$$

$$\hat{B} = \mathrm{diag}\left(\sqrt{2q/\tau}, \sqrt{2q_1 a_1 b_1^2/\tau_1}, \dots, \sqrt{2q_n a_n b_n^2/\tau_n}\right). \tag{4}$$

Here the τ_is, the b_is, and the a_is are positive parameters with the dimension of time, time, and inverse squared time, respectively. We consider ω odd and the Ω_is even under time reversal. With this choice the fluctuating entropy production takes the form of heat exchanges over effective temperatures (see Appendix A 2). We also propose a physical interpretation of the time-reversal symmetries in Appendix A 4. We note that $\hat{A}$ is an arrowhead matrix, namely, it has nonzero elements only in the first row, in the first column, and in the principal diagonal. This form has a physical meaning: The auxiliary variables describe the memory in the system, and each one has a characteristic relaxation time τ_i and is coupled with the main observable only. The above equations are indeed equivalent to the following GLE [19]:

$$\dot{\omega}(t) = -\int_{-\infty}^{t} \gamma(t-t')\omega(t')dt' + \eta_s(t) + F_{\rm ext}, \tag{5}$$

$$\gamma(t) = \frac{2}{\tau}\delta(t) + \sum_{k=1}^{n} a_k e^{-\frac{t}{\tau_k}}, \tag{6}$$

$$\langle \eta_s(t)\eta_s(t')\rangle = \frac{2q}{\tau}\delta(|t-t'|) + \sum_{k=1}^{n} q_k a_k e^{-\frac{|t-t'|}{\tau_k}}, \tag{7}$$

and the auxiliary variables are

$$\Omega_k = -b_k \int_{-\infty}^{t} dt' e^{-\frac{t-t'}{\tau_k}} \left[a_k \omega(t') - \sqrt{\frac{2q_k a_k}{\tau_k}}\xi_k(t') \right]. \tag{8}$$

Interestingly, a memory kernel, which is a sum of a few exponential decays can approximate also nonexponential kernels, such as power-law decays typical of several transport phenomena in dense systems [33] (see also Appendix E). We recall here that the use of exponential memory kernels to describe the diffusion of an intruder in a complex fluid is motivated by a typical approximation done for Brownian motion at high densities when the coupling with hydrodynamic modes decaying exponentially in time is taken into account [27,34].

We point out that this model is built in such a way to recover the fluctuation-dissipation relation of the second kind $\langle \eta_s(t)\eta_s(t')\rangle = q\gamma(|t-t'|)$ if all the thermostats are at the same temperature $q_k = q$. With this condition (and $F_{\rm ext} = 0$), thermodynamic equilibrium is properly described. In the Fokker-Planck formalism this is equivalent to a null irreversible current [35] (see also Appendix A 3). The solution for the stationary probability distribution function is a multivariate Gaussian $P(\boldsymbol{X}) \propto \exp(-\Delta\boldsymbol{X}\hat{\beta}\Delta\boldsymbol{X}/2)$, where $\Delta\boldsymbol{X} = \boldsymbol{X} - \langle\boldsymbol{X}\rangle$ and $\hat{\beta}$ is the inverse of the covariance matrix $\sigma_{ij} = \langle\Delta X_i \Delta X_j\rangle$. Note that thanks to the linearity of the model, $\hat{\beta}$ and $\hat{\sigma}$ do not depend on $F_{\rm ext}$. Such a distribution is canonical ($\beta_{ij} \propto \delta_{ij}/q$) at equilibrium (see Appendix A 1). We remark that the model has two different sources of nonequilibrium: The coupling with different thermal baths (i.e., when q, q_k are different) and the external force $F_{\rm ext}$. Interestingly, the second ingredient triggers an average drift $\langle\boldsymbol{X}\rangle \neq 0$, while the first one does not.

The entropy production rate (EPR) [36] of the model in the steady state reads (see A 2 for details)

$$\langle \dot{S}\rangle = \langle \dot{S}\rangle_{\rm ext} + \langle \dot{S}\rangle_{\rm th}, \tag{9}$$

where we defined an external contribution due to the presence of forcing $\langle \dot{S}\rangle_{\rm ext} = \frac{1}{q}\langle\omega\rangle F_{\rm ext} + \sum_i (\frac{1}{q} - \frac{1}{q_i})\frac{\langle\omega\rangle\langle\Omega_i\rangle}{b_i}$ and one $\langle \dot{S}\rangle_{\rm th} = \sum_i \frac{1}{b_i}(\frac{1}{q} - \frac{1}{q_i})\sigma_{0i}$ due only to the coupling with baths at different temperatures. This last term is positive because it is the only contribution in the absence of the external driving [37]. The mean values of the dynamical variables in the steady state are

$$\langle\omega\rangle = \frac{F_{\rm ext}\tau}{1 + \tau\sum_k \tau_k a_k}, \quad \langle\Omega_i\rangle = -\tau_i a_i b_i \langle\omega\rangle, \tag{10}$$

which implies that $\langle \dot{S}\rangle_{\rm ext}$ is proportional to $F_{\rm ext}^2$.

III. TUR IN THE LARGE TIME LIMIT

We start by considering the bound for the diffusion coefficient of the tracer obtained from the TUR [9,11], valid for overdamped dynamics in the large time limit of the stationary state,

$$\lim_{t\to\infty} \frac{\langle\Delta\theta(t)^2\rangle}{t} \geqslant \frac{2\langle\omega\rangle^2}{\langle \dot{S}\rangle}, \tag{11}$$

where $\Delta\theta(t)$ is defined as in Eq. (1). In our model all the terms of the above inequality can be explicitly computed. Indeed,

we can relate the spectrum and the diffusion coefficient with the Wiener-Khinchin theorem $\mathcal{S}_{00}(0) = \lim_{t\to\infty}\langle\Delta\theta(t)^2\rangle/t$, where the spectral matrix is defined as the Fourier transform of the stationary correlation matrix:

$$\hat{\mathcal{S}}(f) \equiv \int_{-\infty}^{+\infty} dt e^{-ift}\hat{\sigma}(t) = (\hat{A} + i\hat{I}f)^{-1}\hat{B}\hat{B}^T(\hat{A}^T - i\hat{I}f)^{-1}, \tag{12}$$

where $\sigma_{ij}(t-s) = \langle\Delta X_i(t)\Delta X_j(s)\rangle$, and $\hat{I}$ is the identity matrix. Inverting the arrowhead matrix $\hat{A}$ [38], we get (see Appendix A 5)

$$\mathcal{S}_{00}(0) = [\hat{A}^{-1}\hat{B}\hat{B}^T(\hat{A}^T)^{-1}]_{00} = \mathcal{D}_{\rm eq}\left[\frac{1+\tau\sum_k \frac{q_k}{q}a_k\tau_k}{1+\tau\sum_k a_k\tau_k}\right], \tag{13}$$

where $\mathcal{D}_{\rm eq} = 2q\tau/(1+\tau\sum_k a_k\tau_k)$ is the diffusion coefficient when $q_i = q\ \forall\ i$. Then, using Eqs. (9) and (10), we have

$$\frac{2\langle\omega\rangle^2}{\langle\dot{S}\rangle_{\rm ext}} = \mathcal{D}_{\rm eq}\left[\frac{1+\tau\sum_k a_k\tau_k}{1+\tau\sum_k \frac{q}{q_k}a_k\tau_k}\right]. \tag{14}$$

From this expression we arrive to the following relation (see Appendix A 6 for details):

$$\lim_{t\to\infty}\frac{\langle\Delta\theta(t)^2\rangle}{t} \geqslant \frac{2\langle\omega\rangle^2}{\langle\dot{S}\rangle_{\rm ext}} \geqslant \frac{2\langle\omega\rangle^2}{\langle\dot{S}\rangle}. \tag{15}$$

This shows that in our model a bound tighter than that of Eq. (11) can be obtained by considering in the EPR the contribution $\langle\dot{S}\rangle_{\rm ext}$ only. Below we extend this result to finite times.

As an additional remark, we note that completely ignoring the presence of thermostats with different temperatures can imply a violation of the associated inequality. Indeed, defining the contribution associated with the drift $\langle\dot{S}\rangle_{\rm drift} = \langle\omega\rangle F_{\rm ext}/q$, one can verify that the inequality $\mathcal{S}_{00}(0) \geqslant 2\langle\omega\rangle^2/\langle\dot{S}\rangle_{\rm drift} = \mathcal{D}_{\rm eq}$ is violated if $\sum_k(q_k - q)a_k\tau_k < 0$.

IV. TUR AT FINITE TIMES

To derive the general finite-times expression of a TUR with a tighter bound, we can proceed as in [13]. We consider a fictive h dynamics (generating $\langle\cdots\rangle_h$ averages over a distribution P_h) that coincides with the original one as $h = 0$ and write the Cramér-Rao inequality for an unbiased estimator Θ of a function $\psi(h)$:

$$\frac{{\rm Var}_h(\Theta[\Gamma_t])}{[\partial_h\langle\Theta[\Gamma_t]\rangle_h]^2} \geqslant \frac{1}{\mathcal{I}_{\rm F}(h)}. \tag{16}$$

Here Γ_t is the stochastic trajectory of duration t along which the estimator is evaluated and $\mathcal{I}_{\rm F}$ is the Fisher information [39]. Thus we have $\langle\Theta[\Gamma_t]\rangle_h = \psi(h)$, and we require that $(\partial_h\langle\Theta[\Gamma_t]\rangle_h)|_{h=0} = \langle\Theta[\Gamma_t]\rangle$, so that the left-hand side of Eq. (16) calculated in $h = 0$ coincides with the uncertainty of the generalized current $\langle\Theta[\Gamma_t]\rangle$. Note that this condition depends both on how the current is defined and on the choice of the fictive dynamics [12,24].

To derive the TUR with the tighter bound, we introduce a perturbation to Eq. (2) in the form $h\boldsymbol{V}$, where $\boldsymbol{V} = \{\langle\omega\rangle/\tau, -\langle\Omega_1\rangle/\tau_1, \ldots, -\langle\Omega_n\rangle/\tau_n\}$. With this choice, evaluating the Cramér-Rao inequality for $h = 0$ in the stationary state, we get (see Appendix B for details)

$$\frac{\langle\Delta\theta(t)^2\rangle}{(\langle\omega\rangle t)^2} \geqslant \frac{2}{\Delta S_{\rm ext}(t) + \mathcal{I}}, \tag{17}$$

where

$$\mathcal{I} = 2\int d\boldsymbol{X}\frac{[\partial_h P_h(\boldsymbol{X})]^2|_{h=0}}{P(\boldsymbol{X})}, \tag{18a}$$

$$\Delta S_{\rm ext}(t) = \int_0^t dt'\left[\frac{\langle\omega\rangle^2}{\tau q} + \sum_i \frac{\langle\Omega_i\rangle^2}{\tau_i q_i a_i b_i^2}\right] = \langle\dot{S}\rangle_{\rm ext}t. \tag{18b}$$

The above expression coincides with the definition of $\langle\dot{S}\rangle_{\rm ext}$ below Eq. (9) (see Appendix B 2). We then obtain the following TUR for the MSD, also valid at finite times in the steady state, that is consistent with the improved bound discussed for large times, Eq. (15):

$$\langle\Delta\theta(t)^2\rangle \geqslant \frac{2\langle\omega\rangle^2 t^2}{\langle\dot{S}\rangle_{\rm ext}t + \mathcal{I}}. \tag{19}$$

Exploiting the linearity of the model we can easily obtain P_h from which we compute the explicit form of the nonextensive term:

$$\mathcal{I} = 2\langle\omega\rangle^2\beta_{00}. \tag{20}$$

It is important to note that $\langle\omega\rangle^2$ simplifies in the right-hand side of the TUR (19), making it independent of $F_{\rm ext}$, as the left-hand side. Thus for $F_{\rm ext} \to 0$, the bound remains finite, at variance with the weaker bound obtained from the total EPR $\langle\dot{S}\rangle$. Equation (19) therefore also works in the case of force-free diffusion, as shown in the following. We remark that even if the model is linear, an analytical form for the MSD when $n > 1$ can be quite involved [16]. A bound with a simple functional form as the one provided by formula (19) can be, therefore, precious. It is interesting to consider also the consequence of some lack of information in the modeling procedure: for instance, one could overlook the different thermostats and could be tempted to use the asymptotic bound considering just $\langle\dot{S}\rangle_{\rm drift}$ for the whole available time range (which is appealing as it is simpler and does not require estimating $\mathcal{I}$). We denote this case as the "incomplete bound" (IB) and discuss its consequences in the following examples.

V. TRACER DYNAMICS IN A DENSE GRANULAR MEDIUM

In order to illustrate the validity of our results and to show their relevance in physical systems, we apply them in the case of diffusion in driven granular fluids. We consider the case $n = 1$, that has been shown to describe the behavior of a massive tracer in a moderately dense granular medium [27]. In this conditions the MSD of the tracer can exhibit a subdiffusive behavior at intermediate times due to the caging effect of the surrounding grains. We compare the bound (19) with MSD of this kind obtained in experiments [4] and molecular dynamics simulations [27]. In the experiment, the tracer diffuses in a system of steel spheres confined in a three-dimensional (3D)

box vertically driven by an electrodynamic shaker, while numerical simulations consider the two-dimensional (2D) case of hard dissipative disks coupled to a spatially homogeneous thermostat. We use the 2D form of Eq. (2) with $a_1 = \frac{\alpha}{\tau\tau_1}$ and $b_1 = \tau$ obtaining the same model used in [27]. The mean values $\langle\omega\rangle = \tau F_{\rm ext}/(1+\alpha)$ and $\langle\Omega_1\rangle = -\alpha\langle\omega\rangle$ appear in the EPR:

$$\langle\dot{S}\rangle = \frac{1}{q}\langle\omega\rangle F_{\rm ext} - \left[\frac{q_1 - q}{\tau q q_1}\right]\alpha\langle\omega\rangle^2 + \left[\frac{q_1 - q}{\tau q q_1}\right]\hat{\sigma}_{01}. \quad (21)$$

The comparison of the bounds discussed above with the MSD measured in experiments and simulations is shown in Fig. 1(a). Here we see that the bound from Eq. (19) (dashed lines) is close (from below) to the data at all timescales. The IB (dot-dashed lines) is obtained neglecting the different thermostats. Two possible situations may appear: (i) the IB is valid at late times but (as expected) violated at short times (see curves for the 2D simulations), (ii) it is violated also in the diffusive regime (see data for the 3D experiment). The difference between these two conditions depends on the interplay of characteristic times and temperatures. Since data come from force-free diffusion, we used the bound in the limit $F_{\rm ext} \to 0$, which is meaningful for Eq. (19) while trivial for Eq. (11). This is the reason why we don't compare our bound with that obtained from the standard TUR in Fig. 1(a).

The bound on the extent of nondiffusive regimes of our model is discussed in Appendix D. We stress that a valid TUR without the hypothesis of velocity relaxation is necessary in this class of model because, contrary to what happens in [15], the MSD predicted by our model always exhibits a ballistic regime at short times. Then, in order to correctly bound the extent of anomalous diffusion, we need a thermodynamic bound that is not simply linear in time.

VI. FORBIDDEN EQUILIBRIUM REGIMES

The derived bound Eq. (19) holds on a class of models for which the analytical expression of many thermodynamic quantities is available [16,35]. Thus it is important to specify for which practical purpose one can exploit our bound. In view of this, here we show how Eq. (19) can be used to directly infer nonequilibrium signatures from data. We consider the right-hand side of Eq. (19) at equilibrium and we refer to it as $\mathcal{B}_{\rm eq}(t)$. We equate all the thermostats in Eqs. (14) and (13) and take $\hat{\sigma}$ diagonal in Eq. (20), obtaining

$$\mathcal{B}_{\rm eq}(t) \sim \langle\Delta\theta(t)^2\rangle \sim \begin{cases} \langle\Delta\omega^2\rangle t^2 & t \ll \mathcal{I}/\langle\dot{S}\rangle_{\rm ext} \\ \mathcal{D}_{\rm eq} t & t \gg \mathcal{I}/\langle\dot{S}\rangle_{\rm ext}. \end{cases} \quad (22)$$

Note that $\mathcal{I}/\langle\dot{S}\rangle$ is always well defined at equilibrium since the quadratic dependence on $F_{\rm ext}$ cancels out. Provided that the system is in equilibrium, Eq. (22) shows that the MSD and the bound coincide in both the short and long time limit, while for intermediate times the inequality holds. This observation allows one to exclude the occurrence of certain transient anomalous diffusion regimes at equilibrium or, equivalently, to ensure that certain forms of MSD are compatible only with

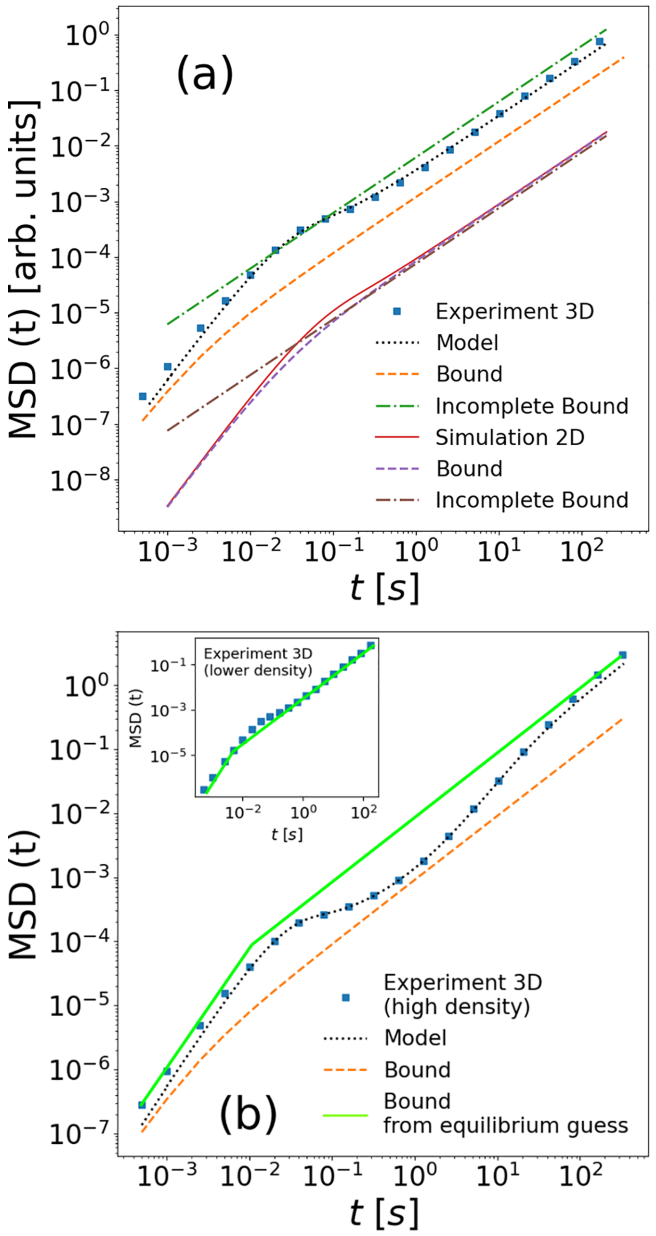

FIG. 1. MSD of a large intruder immersed in a vibrated granular fluid at moderate density (a) and at high density (b). In both cases the bounds are calculated with the numerical values of the model parameters obtained by fitting the data. Details on the fitting procedure are given in Appendix C. In panel (b), the equilibrium guess is constructed by connecting the two slopes of the ballistic and the diffusive regime following what we would expect at equilibrium from Eq. (22). The inset shows an MSD [same experimental data of panel (a)] whose form is compatible with thermodynamic equilibrium.

nonequilibrium dynamics. This test for equilibrium compatibility can be done by connecting the two slopes of the ballistic and diffusive regimes of a given MSD in a log-log plot and considering this curve as a lower bound from an equilibrium guess. Indeed, given the functional form of the bound Eq. (19) and knowing that it reduces to an equality at short and long times if $q_i = q \ \forall \ i$ [Eq. (22)], an MSD coming from an equilibrium dynamics is expected to lie above the constructed curve at all times. Then, when any tract of the MSD is found

to lie below the lower bound from the equilibrium guess, then one can deduce that if the dynamics follows Eqs. (2) and (4), the observed MSD is not compatible with thermodynamic equilibrium. To illustrate this application, we consider the case $n = 2$ that can describe the anomalous diffusion of a tracer in a dense granular system with very slow characteristic times. We take $a_1 = \frac{\alpha}{\tau\tau_1}$, $a_2 = \frac{\epsilon^2}{\tau\tau_2}$, and $b_1 = b_2 = \tau$, where $\epsilon = \tau/\tau_2$. For $\epsilon \to 0$ and keeping finite the amplitude of the noise ξ_2, we obtain the same model described in [5]. As we can see in Fig. 1(b), this model can properly reproduce the experimental data of the MSD, characterized by a surprising superdiffusive regime after the cage subdiffusion. Its origin relies on the presence of a slow collective motion of the granular medium due to the interplay of disorder and friction [6,40]. As evident from Fig. 1(b), the behavior of the MSD is not compatible with the bound guessed from the equilibrium condition (22). Then we can conclude that the underlying dynamics is out of equilibrium without performing any further analysis. In order to complete the picture, we show in the inset of Fig. 1(b) the application of this procedure to the experimental data of Fig. 1(a), which come from a less dense system where the slow collective motion and the consequent superdiffusive regime do not appear. In this case the MSD always lies above the equilibrium guess, so we cannot draw any conclusion on the nonequilibrium properties of the dynamics without estimating the model's parameters.

We point out that the proposed test for equilibrium compatibility is especially relevant in the recent debate on the possibility to deduce the nonequilibrium character of a system from partial observation [8], in particular, recalling that the time series of a scalar Gaussian process [in our case $\omega(t)$] is always symmetric under time reversal [41,42].

VII. CONCLUSIONS

TURs represent an impressive result with manifold applications, from the evaluation of the entropic cost for the precision ratio of currents [43], to the estimation of entropy production [44] in nonequilibrium systems, to the identification of limits on the temporal regimes of anomalous diffusion [15]. Considering a class of generalized Langevin equations with several exponential timescales and uniform external force, we have derived a bound for the MSD [Eq. (19)] which improves the one obtained through the standard TUR [Eq. (11)]. Indeed, our bound is tighter, valid at all times, and useful also for freely diffusing particles. The class of linear models we considered can describe the coupling between relevant degrees of freedom in many-body interacting systems. This allowed us to test our results on experimental and numerical data of a tracer diffusing in a granular medium. Moreover, we showed how to use this bound as an immediate tool for inferring nonequilibrium properties of the dynamics from the shape of the MSD. Our approach can be extended to other nonequilibrium systems where several sources of dissipation are present, such as fluids of active particles or driven mixtures. We also recall that linearly coupled equations are the natural framework of linear irreversible thermodynamics, valid (at small perturbations) also for periodically forced systems [45]. The generalization of our results to nonlinear cases such as particles subjected to periodic potentials or nonlinear frictional forces represents a promising perspective.

ACKNOWLEDGMENTS

The authors acknowledge financial support from the MIUR PRIN2017 project through Grant No. 201798CZLJ. A.P. acknowledges financial support from Labex Palm (Project FT2AC). The Authors wish to thank Hyunggyu Park for interesting discussions.

APPENDIX A: DETAILS OF CALCULATIONS FOR THE GENERAL MODEL

In this section we report the calculations necessary to obtain some relevant quantities that are used in the main text. For clarity reasons we rewrite here the definition of the general model. We consider the multivariate linear stochastic differential equation (SDE) $\dot{\boldsymbol{X}} = \hat{A}\boldsymbol{X} + \hat{B}\boldsymbol{\xi} + \boldsymbol{F}$, where $\boldsymbol{X} = \{\omega, \Omega_1, \ldots, \Omega_n\}$, $\boldsymbol{\xi} = \{\xi_0, \xi_1, \ldots, \xi_n\}$, and $\boldsymbol{F} = \{F_{\text{ext}}, 0, \ldots, 0\}$. The interaction and the noise matrices are give by

$$\hat{A} = \begin{pmatrix} -1/\tau & 1/b_1 & \ldots & 1/b_n \\ -a_1 b_1 & -1/\tau_1 & 0 & 0 \\ \vdots & 0 & \ddots & 0 \\ -a_n b_n & 0 & 0 & -1/\tau_n \end{pmatrix}, \tag{A1}$$

$$\hat{B} = \text{diag}\left(\sqrt{2q/\tau}, \sqrt{2q_1 a_1 b_1^2/\tau_1}, \ldots, \sqrt{2q_n a_n b_n^2/\tau_n}\right). \tag{A2}$$

All the model parameters are assumed to be positive. As in the main text, we define $\Delta\boldsymbol{X} = \boldsymbol{X} - \langle \boldsymbol{X} \rangle$, $\hat{\beta} = \hat{\sigma}^{-1}$, and $\sigma_{ij} = \langle \Delta X_i \Delta X_j \rangle$.

1. Stationary probability distribution function

The stationary probability distribution function of the model is the multivariate Gaussian [35] $P(\boldsymbol{X}) \propto \exp(-\frac{1}{2}\Delta\boldsymbol{X}\hat{\beta}\Delta\boldsymbol{X})$. To have an explicit expression of that, one has to solve the following equation for the covariance matrix $\hat{\sigma}$:

$$\hat{A}\hat{\sigma} + \hat{\sigma}\hat{A}^T = -\hat{B}\hat{B}^T. \tag{A3}$$

The solution of such a matrix equation for our model in the general case is cumbersome. Here we report the explicit solution for $n = 1$:

$$\hat{\sigma} = \frac{1}{(1 + a_1\tau\tau_1)(\tau + \tau_1)} \begin{pmatrix} a_1 q_1 \tau^2 \tau_1 + q\left(\tau + \tau_1 + a_1 \tau \tau_1^2\right) & a_1 b_1 \tau \tau_1 (q_1 - q) \\ a_1 b_1 \tau \tau_1 (q_1 - q) & a_1 b_1 \left[a_1 q \tau \tau_1^2 + q_1(\tau + \tau_1 + a_1 \tau^2 \tau_1)\right] \end{pmatrix}. \tag{A4}$$

Our model is built in such a way to have thermodynamic equilibrium if $q_i = q\ \forall i$ and $F_{\text{ext}} = 0$. In such a condition we expect the equilibrium probability distribution function to be canonical (i.e., $\hat{\beta}_{ij}^{\text{eq}} \propto \delta_{ij}/q$). Now we check that by Eq. (A3).

We assume $\hat{\sigma}^{\rm eq}_{ij} = c_i\delta_{ij}$ and substitute it into Eq. (A3) with $q_i = q$:

$$(\hat{A}\hat{\sigma}^{\rm eq} + \hat{\sigma}^{\rm eq}\hat{A}^T)_{ij} = A_{ij}c_j + c_iA^T_{ij} = -\left(B^{\rm eq}_{ii}\right)^2\delta_{ij}. \tag{A5}$$

For $i = j = 0$ we have $c_0 = -B^2_{00}/A_{00} = 2q$, while if $i = j \neq 0$ one has $c_i = -(B^{\rm eq}_{ii})^2/A_{ii} = 2qa_ib_i^2$. With this solution, is easy to verify that the left-hand side of Eq. (A5) is always zero if $i \neq j$. The equilibrium probability distribution function is then given by

$$P_{\rm eq}(\boldsymbol{X}) \propto \exp\left[-\frac{1}{2q}\left(\omega^2 + \sum_{i=1}^{n}\frac{\Omega_i^2}{a_ib_i^2}\right)\right]. \tag{A6}$$

2. Entropy production

We consider the entropy production of the general model defined according to the Lebowitz and Spohn functional. We use the relation reported in [19] that expresses the entropy production as the product of reversible and irreversible components of the drift in the Langevin equation. Since we are interested in the entropy production in the stationary state, we only consider the term that is extensive in time. We obtain

$$\Delta S(t) = \log\frac{\text{Prob}\left(\{\omega(s), \Omega_1(s), \dots \Omega_n(s)\}_0^\tau\right)}{\text{Prob}\left(\{-\omega(t-s), \Omega_1(t-s), \dots, \Omega_n(t-s)\}_0^t\right)} \tag{A7}$$

$$= \frac{1}{D_\omega}\int_0^t ds\left[A^{\rm irr}_\omega(\dot{\omega}(s) - A^{\rm rev}_\omega)\right] + \sum_{i=1}^{n}\frac{1}{D_{\Omega_i}}\int_0^t ds\left[A^{\rm irr}_{\Omega_i}(\dot{\Omega}_i(s) - A^{\rm rev}_{\Omega_i})\right], \tag{A8}$$

where $D_\omega = q/\tau$, $D_{\Omega_i} = q_ia_ib_i^2/\tau_i$, and

$$A^{\rm rev}_\omega = \sum_{i=1}^{n}\frac{\Omega_i(s)}{b_i} + F_{\rm ext}, \quad A^{\rm irr}_\omega = -\frac{\omega(s)}{\tau},$$
$$A^{\rm rev}_{\Omega_i} = -a_ib_i\omega(s), \quad A^{\rm irr}_{\Omega_1} = -\frac{\Omega_i(s)}{\tau_i}, \tag{A9}$$

having used the fact that ω is odd and the Ω_is are even under time reversal (see Appendix A 4 below). Therefore, for the entropy production in the stationary state, we obtain

$$\Delta S(t) = \frac{1}{D_\omega}\int_0^t ds\left(-\frac{\omega(s)}{\tau}\right)\left[\dot{\omega}(s) - \sum_{i=1}^{n}\frac{\Omega_i(s)}{b_i} - F_{\rm ext}\right] + \sum_{i=1}^{n}\frac{1}{D_{\Omega_i}}\int_0^t ds\left(-\frac{\Omega_i(s)}{\tau_i}\right)[\dot{\Omega}_i(s) + a_ib_i\omega(s)] \tag{A10}$$

$$= \frac{1}{D_\omega}\left[-\frac{\delta\omega^2}{2\tau} + \frac{1}{\tau}\int_0^t ds\,\omega(s)\left(\sum_{i=1}^{n}\frac{\Omega_i(s)}{b_i} + F_{\rm ext}\right)\right] + \sum_{i=1}^{n}\frac{1}{D_{\Omega_i}}\left[-\frac{\delta\Omega_i^2}{2\tau_i} - \frac{a_ib_i}{\tau_i}\int_0^t ds\,\omega(s)\Omega_i(s)\right] \tag{A11}$$

$$= -\frac{\delta_t(\omega^2)}{2q} - \sum_{i=1}^{n}\frac{\delta_t\left(\Omega_i^2\right)}{2q_ia_ib_i^2} + \frac{1}{q}\int_0^t ds\,\omega(s)F_{\rm ext} + \sum_{i=1}^{n}\frac{1}{b_i}\int_0^t ds\left(\frac{1}{q} - \frac{1}{q_1}\right)\omega(s)\Omega_i(s), \tag{A12}$$

where we introduced the notation $\delta_t(z) = z(t) - z(0)$. Considering that in the stationary state we expect $\langle\Delta S(t)\rangle = \langle\dot{S}\rangle t$, the average entropy production rate is then

$$\langle\dot{S}\rangle = \frac{1}{q}\langle\omega\rangle F_{\rm ext} + \sum_{i=1}^{n}\frac{1}{b_i}\left(\frac{1}{q} - \frac{1}{q_i}\right)\langle\omega\rangle\langle\Omega_i\rangle + \sum_{i=1}^{n}\frac{1}{b_i}\left(\frac{1}{q} - \frac{1}{q_i}\right)\sigma_{0i}, \tag{A13}$$

which coincides with the expression reported in Eq. (9) of the main text. It is also important to note that Eq. (A12) is consistent with thermodynamic interpretation for which, at equilibrium, the only contribution to the fluctuating entropy production is the work done by the thermal bath. Indeed, rescaling the auxiliary variables as $\tilde{\Omega}_i = \Omega_i/\sqrt{a_ib_i^2}$, one obtains

$$\Delta S^{\rm eq}(t) = -\frac{\delta_t(\omega^2)}{2q} - \sum_{i=1}^{n}\frac{\delta_t\left(\tilde{\Omega}_i^2\right)}{2q}, \tag{A14}$$

which is evidently zero when averaged on the stationary state. The interpretation of the above expression as the total fluctuating work done by the thermostats is consistent with the equilibrium probability distribution function [Eq. (A6)].

3. Equilibrium condition for the Fokker-Planck equation

The Fokker-Planck equation associated with Eq. (2) reads

$$\partial_tP(\boldsymbol{X}, t) = -\nabla\cdot[\boldsymbol{J}^{\rm rev}(\boldsymbol{X}, t) + \boldsymbol{J}^{\rm irr}(\boldsymbol{X}, t)], \tag{A15}$$

where

$$J^{\rm irr}_i(\boldsymbol{X}, t) = \left[A^{\rm irr}_i(\boldsymbol{X}, t) - \frac{1}{2}B^2_{ii}\partial_{X_i}\right]P(\boldsymbol{X}, t) \tag{A16}$$

$$J^{\rm rev}_i(\boldsymbol{X}, t) = A^{\rm rev}_i(\boldsymbol{X}, t)P(\boldsymbol{X}, t). \tag{A17}$$

From Eqs. (A2) and (A9) it is easy to check that, as we expect, the probability distribution function given by Eq. (A6) makes the irreversible current $J^{\rm irr}_i(\boldsymbol{X}, t)$ equal to zero when $q_i = q\ \forall i$.

4. Symmetry under time reversal of the auxiliary variables

The calculations done so far assume the auxiliary variables to be even under time reversal. This is a forced choice if we want to obtain the correct thermodynamic interpretation expressed by Eq. (A14). Nevertheless, this choice may seem unphysical because in our model the Ω_is and ω can have the same physical dimensions (see Appendix C below), so one expects them to follow the same symmetry under time reversal. Here we want to provide an argument that clarifies why considering even Ω_is is actually reasonable from a physical point of view. Let us consider a particular case of our general

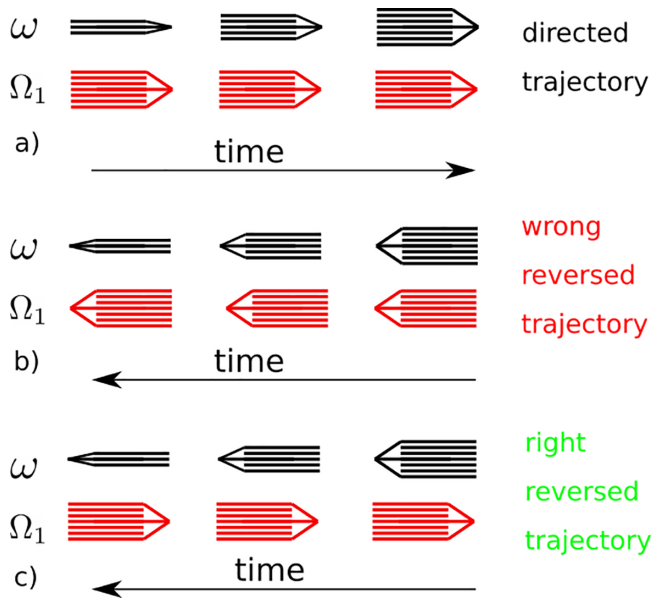

FIG. 2. Evolution of ω and Ω_1, the arrow width corresponds to vector magnitude. (a) Directed trajectories of ω and Ω_1: the auxiliary variable increases the intruder's velocity. We consider a limit in which Ω_1 is not perturbed by the intruder to ease the readability of the cartoon. (b) Reversed trajectories with both the variables considered odd under time reversal. Here the auxiliary field would naturally increase the intruder's velocity, so the observed slowing down is entirely originated by the action of noise. (c) Reversed trajectories considering ω odd and Ω_1 even under time reversal. The auxiliary variable increases the intruder's velocity with the same probability.

model where $n = 1, q = q_1, \alpha = 0, F_{\rm ext} = 0$, and $\tau_1 \gg \tau$. The equations of motion then read

$$\dot{\omega} = -\frac{1}{\tau}(\omega - \Omega_1) + \sqrt{\frac{2q}{\tau}}\xi_0, \quad \dot{\Omega}_1 = 0. \tag{A18}$$

These equations represent the diffusion of an intruder (ω) in a fluid with a local velocity field (Ω_1) that relaxes on timescales much larger than τ. If the two variables have the same(opposite) sign, the velocity field fastens(slows down) the intruder. Being a subcase of the general model with $q = q_1$ (i.e., thermodynamic equilibrium), we expect for the trajectories of $\{\omega(t), \Omega_1(t)\}$ to have the same probability under time reversal. In Fig. 2 we show one possible directed evolution of the two variables and the comparison between time-reversal operations where Ω_1 is considered odd or even. It is clear that the case in which Ω_1 is odd (b) requires a (very improbable) realization of the noise that is able to slow down ω despite the positive contribution of Ω_1. On the contrary, it is reasonable to think that the reversed trajectories with even Ω_1 (c) can be obtained with a realization of the noise that has the same probability of the directed one. The conclusion we draw from this cartoon is that we must consider auxiliary variables as external fields. Thus we do not change their sign under time reversal, even if they have the same physical dimension of a velocity and they are influenced by the intruder dynamics.

5. Diffusion coefficient

To obtain a general expression of the diffusion coefficient of our model, $\lim_{t\to\infty}\langle\Delta\theta(t)^2\rangle/t = \mathcal{S}_{00}(0) = [\hat{A}^{-1}\hat{B}\hat{B}^T(\hat{A}^T)^{-1}]_{00}$, one needs to invert the arrowhead matrix $\hat{A}^T$. We first perform the matrix product and get

$$[\hat{A}^{-1}\hat{B}\hat{B}^T(\hat{A}^T)^{-1}]_{00} = \sum_{kj} A^{-1}_{0j}B^2_{jj}\delta_{jk}A^{-1}_{0k} = \sum_k \left(A^{-1}_{0k}B_{kk}\right)^2, \tag{A19}$$

where the sums run from 0 to $n+1$ and δ_{jk} is the Kronecker delta. From Ref. [38] we know that

$$\det(A)A^{-1}_{00} = (-1)^n\prod_{j=1}^n\frac{1}{\tau_j}, \quad \det(A)A^{-1}_{0k} = (-1)^n\frac{\tau_k}{b_k}\prod_{j=1}^n\frac{1}{\tau_j},$$
$$\det(A) = (-1)^{n+1}\prod_{j=1}^n\frac{1}{\tau_j}\left[\frac{1}{\tau} + \sum_{i=1}^n a_i\tau_i\right], \tag{A20}$$

and with some algebraic manipulation we arrive at

$$\mathcal{S}_{00}(0) = \mathcal{D}_{\rm eq}\left[\frac{1+\tau\sum_k\frac{q_k}{q}a_k\tau_k}{1+\tau\sum_k a_k\tau_k}\right], \tag{A21}$$

which coincides with Eq. (13) of the main text.

6. TUR in the large time limit

The TUR valid at large times reported in Eq. (15) of the main text has been derived by directly evaluating the quantities involved in it from the general model:

$$\lim_{t\to\infty}\frac{\langle\Delta\theta(t)^2\rangle}{t} \geqslant \frac{2\langle\omega\rangle^2}{\langle\dot{S}\rangle_{\rm ext}} \geqslant \frac{2\langle\omega\rangle^2}{\langle\dot{S}\rangle}. \tag{A22}$$

The first inequality follows from verifying that

$$\left[\frac{1+\tau\sum_k\frac{q_k}{q}a_k\tau_k}{1+\tau\sum_k a_k\tau_k}\right] - \left[\frac{1+\tau\sum_k a_k\tau_k}{1+\tau\sum_k\frac{q}{q_k}a_k\tau_k}\right]$$
$$= \tau\sum_k\frac{a_k\tau_k}{qq_k}(q-q_k)^2 + \tau^2\sum_{j>k}\frac{\tau_j a_j\tau_k a_k}{q_k q_j}(q_j-q_k)^2 \geqslant 0. \tag{A23}$$

The second inequality of (A22) is directly related to the decomposition of the entropy production rate $\langle\dot{S}\rangle = \langle\dot{S}\rangle_{\rm ext} + \langle\dot{S}\rangle_{\rm th}$ and the positivity of $\langle\dot{S}\rangle_{\rm th}$. We recall that $\langle\dot{S}\rangle_{\rm th} = \sum_i\frac{1}{b_i}(\frac{1}{q}-\frac{1}{q_i})\hat{\sigma}_{0i} \geqslant 0$ follows from the fact that in the absence of external force it is the only contribution to the entropy production rate and that its expression does not depend on $F_{\rm ext}$ thanks to the linearity of the model.

APPENDIX B: UNDERDAMPED TUR FROM CRAMÉR-RAO INEQUALITY

1. Relation with previously derived TUR

The derivation of the TUR in the large time limit has been performed exploiting the fact that it is possible to derive an explicit and compact expression for both the diffusion coefficient [Eq. (A21)] and the entropy production rate [Eq. (A13)] in our model. Using the same procedure to derive a TUR valid at all timescales is much more complicated, because (i) one has to handle the general expression of the MSD of the model

that is cumbersome, and (ii) one has to guess a time-dependent functional form of the bound.

A TUR valid at all timescales for a general Langevin dynamics with a fully underdamped structure has been derived in [24] following the method explained in [13]. By fully underdamped we mean a system where one half of the degrees of freedom is even under time reversal and is obtained as the derivative of the other half that is odd under time reversal. Such a TUR takes the following form:

$$\frac{\mathrm{Var}(\Theta(t))}{\langle\Theta(t)\rangle^2} \geqslant \frac{1}{\Delta S(t)+\mathcal{I}}, \tag{B1}$$

where $\Theta(t)$ is a generalized integrated current, $\Delta S(t)$ is the *total* entropy production, and $\mathcal{I}$ is a nonextensive term in time. It is worth mentioning that (B1) represents an improvement with respect the underdamped TUR derived in [12] because it has the correct large time limit. With some calculations (not shown) it is possible to show that the same TUR can be derived also for our model that has a partial underdamped structure (i.e., ω is odd and all the Ω_is are even under time reversal). Nevertheless, the above TUR in the large time limit brings an inequality that can be improved by substituting $\Delta S(t)$ with $\Delta S_{\mathrm{ext}}(t)$. As reported in the main text, one of the main results of our work is the derivation of the following TUR:

$$\frac{\langle\Delta\theta(t)^2\rangle}{(\langle\omega\rangle t)^2} \geqslant \frac{2}{\Delta S_{\mathrm{ext}}(t)+\mathcal{I}}. \tag{B2}$$

It is valid at all times in the steady state and brings the improved inequality (A22) in the large time limit.

2. Details of the derivation

In order to derive the TUR (B2) from the Cramér-Rao inequality [Eq. (16) in the main text] we write the SDE of our model with a perturbation depending on the parameter h:

$$dX_i = f_i^h(\boldsymbol{X})dt + B_{ii}dW(t), \tag{B3}$$

where $dW(t)$ is the increment of the Wiener process and

$$f_i^h(\boldsymbol{X}) = \sum_j A_{ij}X_j + F_i + hV_i. \tag{B4}$$

We then apply the main results of Ref. [13]. Considering initial conditions in the steady state, the Fisher information takes the following form:

$$\mathcal{I}_{\mathrm{F}}(h) = -\left\langle\partial_h^2 \ln P_h(\boldsymbol{X})\right\rangle_h + \left\langle\int_0^t dt' \sum_i \left(\frac{\partial_h f_i^h(\boldsymbol{X})}{B_{ii}}\right)^2\right\rangle_h, \tag{B5}$$

where $P_h(\boldsymbol{X})$ is the probability distribution function of the perturbed process and $\langle\cdot\rangle_h$ refers to averages on such a probability. Since the system is linear and the h perturbation does not depend on $\boldsymbol{X}$, the stationary probability distribution associated to the fictive dynamics is still a multivariate Gaussian with the same covariance matrix but different average values $\langle X_i\rangle_h$. Thus, $P_h(\boldsymbol{X}) \propto \exp[(\boldsymbol{X}-\langle\boldsymbol{X}\rangle_h)^T\hat{\beta}(\boldsymbol{X}-\langle\boldsymbol{X}\rangle_h)/2]$. Moreover, from Eq. (B4) one has $\partial_h f_i^h(\boldsymbol{X}) = V_i$. In order to make the Cramér-Rao inequality fully explicit, we then need to compute the average values $\langle X_i\rangle_h$. With the specific choice done in the main text $\boldsymbol{V} = \{\langle\omega\rangle/\tau, -\langle\Omega_1\rangle/\tau_1, \ldots, -\langle\Omega_n\rangle/\tau_n\}$, the following relations must be satisfied:

$$-\frac{1}{\tau}\langle\omega\rangle_h + \sum_i \frac{\langle\Omega_i\rangle_h}{b_i} + F_{\mathrm{ext}} + hV_0 = 0, \tag{B6a}$$

$$-\frac{1}{\tau_i}\langle\Omega_i\rangle_h - a_ib_i\langle\omega\rangle_h - hV_i = 0, \tag{B6b}$$

from which we obtain $\langle\omega\rangle_h = (1+h)\langle\omega\rangle$ and $\langle\Omega_i\rangle_h = \langle\Omega_i\rangle$.

Substituting these relations in the Cramér-Rao inequality for $h=0$ we find the TUR (B2). Indeed, the Fisher information becomes

$$\mathcal{I}_{\mathrm{F}}(0) = \int d\boldsymbol{X}\frac{[\partial_h P_h(\boldsymbol{X})]^2|_{h=0}}{P(\boldsymbol{X})} + \frac{1}{2}\left[\frac{\langle\omega\rangle^2}{\tau q} + \sum_i \frac{\langle\Omega_i\rangle^2}{\tau_i q_i a_i b_i^2}\right]t$$
$$= \frac{1}{2}[\mathcal{I} + \langle\dot{S}\rangle_{\mathrm{ext}}t]. \tag{B7}$$

The relation between the first term of Eq. (B7) and Eq. (20) of the main text follows from the direct evaluation of the probability distribution's derivative with respect h:

$$\int d\boldsymbol{X}\frac{[\partial_h P_h(\boldsymbol{X})]^2|_{h=0}}{P(\boldsymbol{X})} = \left\langle\left[\frac{1}{2}\sum_{jn}\beta_{jn}\partial_h\left(\Delta X_j^h\Delta X_n^h\right)\right]^2\right\rangle$$
$$= \langle\omega\rangle^2\sum_{jn}\beta_{0n}\beta_{0j}\sigma_{nj} = \langle\omega\rangle^2\beta_{00}, \tag{B8}$$

where we used $\Delta X_j^h = (X_j - \langle X_j\rangle_h)$ and $\partial_h\Delta X_j^h = \langle\omega\rangle\delta_{0j}$. Finally, using the relation between $\langle\omega\rangle$ and $\langle\Omega_i\rangle$ [Eq. (10) of the main text], we note that

$$\frac{\langle\omega\rangle^2}{\tau q} = \frac{1}{q}\omega F_{\mathrm{ext}} + \sum_i \frac{\langle\omega\rangle\langle\Omega_i\rangle}{qb_i} \quad \text{and} \quad \frac{\langle\Omega_i\rangle^2}{\tau_i q_i a_i b_i^2} = -\frac{\langle\omega\rangle\langle\Omega_i\rangle}{q_i b_i}. \tag{B9}$$

So, we find that the second term of Eq. (B7) is directly related to the entropy production rate as expressed in Eq. (9).

APPENDIX C: FITTING PROCEDURE

In order to fit the model's parameter, we used two distinct methods for numerical and experimental data. In the numerical data, independent measurements of the autocorrelation and the response function of the granular intruder are available [27]. The model we used for them is defined by the following matrices:

$$\hat{A} = \begin{pmatrix} -1/\tau & 1/\tau \\ -\alpha/\tau_1 & -1/\tau_1 \end{pmatrix}, \quad \hat{B} = \begin{pmatrix} \sqrt{2q/\tau} & 0 \\ 0 & \sqrt{2q_1\alpha\tau/\tau_1^2} \end{pmatrix}, \tag{C1}$$

so it counts five parameters τ, q, α, τ_1, q_1. A multibranch fit of autocorrelation and response allows us to determine the numerical value of such parameters without overfitting. Regarding the experiments performed at moderate density [reported in Fig. 1(a) of the main text], we still use (C1), but here we have only data with which we can reconstruct the autocorrelation, the MSD and the power spectral density of the velocity (PSDV) in the steady state. These are all observables that store the same amount of information in different ways.

Indeed, knowing the autocorrelation function, we can obtain the MSD with Kubo's formula or the PSDV by a Fourier transform. In a linear model with $n+1$ variables, the autocorrelation function is a sum of $n+1$ exponential decays, each one identified by an amplitude and a characteristic time. Thus a fit of the autocorrelation or an equivalent observable alone can be used to estimate a maximum of $2(n+1)$ parameters. In order to have four free parameters, we have fixed $\alpha = 1$ before doing the fit of the experimental data at moderate density. A similar procedure has to be done to fit the experimental data at high density [shown in Fig. 1(b) of the main text]. In this case the matrices of the model are given by

$$\hat{A} = \begin{pmatrix} -1/\tau & 1/\tau & 1/\tau \\ -\alpha/\tau_1 & -1/\tau_1 & 0 \\ -\epsilon^2/\tau_2 & 0 & -1/\tau_2 \end{pmatrix},$$
$$\hat{B} = \begin{pmatrix} \sqrt{2q/\tau} & 0 & 0 \\ 0 & \sqrt{2q_1\alpha\tau/\tau_1^2} & 0 \\ 0 & 0 & \epsilon^{3/2}\sqrt{2q_2/\tau_2} \end{pmatrix}. \quad \text{(C2)}$$

Remembering that $\epsilon = \tau/\tau_2$, we have seven parameters τ, q, α, τ_1, q_1, τ_2, q_2, and in order to not overfit, we fixed $q = q_1$ before doing the fit.

With this fitting procedure we are able to reproduce the MSD and the PSDV (not shown), but dealing with a large number of parameters we know that there is probably an entire region of the parameter space where we could find a good agreement with the experimental data. In view of this, we stress that the important point of our analysis is that there is a set of parameters well reproducing our data for which is important to take into account the correct terms of EPR in the TURs. Nevertheless, it is also important to note that the arbitrariness in the estimation of the model's parameters from data is a quite general issue. In light of this, we remark that the last result presented in the main text (i.e., nonequilibrium signatures in the shape of the MSD) does not require any fit of the data.

APPENDIX D: EXTENT OF THE ANOMALOUS DIFFUSION

Here we want to adapt the analysis done in [15] to the new bound derived in the main text. Considering a regime where the MSD behaves as $\langle \Delta\theta(t)^2 \rangle \sim K_\nu t^\nu$ we have that

$$K_\nu t^\nu \geqslant \frac{C_1 t^2}{1 + C_2 t} \sim \begin{cases} C_1 t^2 & t \to 0 \\ \frac{C_1}{C_2} t & t \to \infty \end{cases}, \quad \text{(D1)}$$

where $C_1 = 2\langle\omega\rangle^2/\mathcal{I}$ and $C_2 = \langle \dot{S} \rangle_{\rm ext}/\mathcal{I}$. The above inequality is satisfied only for times that solve $t^{\nu-2} + C_2 t^{\nu-1} - C_1/K_\nu \geqslant 0$. We can take $\nu = 0$ for an example of the subdiffusive case and $\nu = 2$ for the superdiffusive one, obtaining

$$t^*_{\rm sub} \leqslant \frac{2}{C_2}\left(\sqrt{1 + \frac{4C_1}{C_2^2 K_0}}\right)^{-1}, \quad t^*_{\rm super} \geqslant \frac{1}{C_2}\left(\frac{C_1}{K_2} - 1\right). \quad \text{(D2)}$$

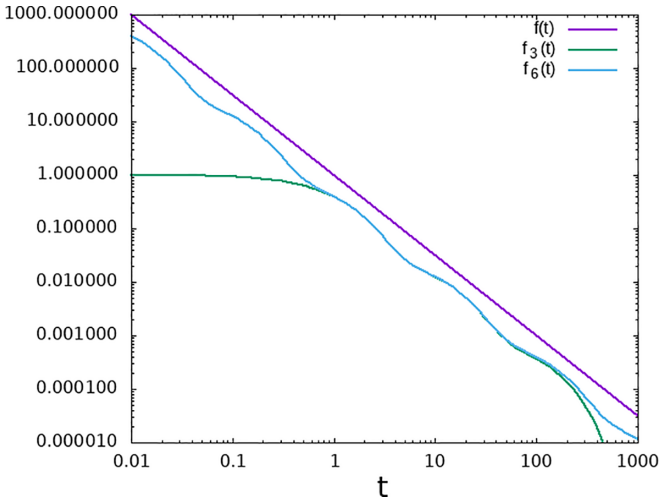

FIG. 3. Comparison between a power-law decay $f(t)$ and two approximations given by the sum of exponentials. See text for the definition of the parameters.

We note that in the subdiffusive case, there is always a positive time that prevents the extension of the subdiffusion after a certain time. On the other hand, the superdiffusive case has a meaningful bound only if $K_2 < C_1$, i.e., if the anomalous diffusion coefficient is lower than the ballistic one of the bound. Having in mind a log-log plot, it means that if the superdiffusive regime $K_2 t^2$ lays over the line $C_1 t^2$ it can hold for any positive times. In the opposite case the onset of such a regime cannot occur before $t^*_{\rm super}$. This is consistent with the fact that the ballistic regime is always present in an underdamped system for $t \sim 0$. The bound applies to the anomalous superdiffusive regimes that may appear at larger times, as the one shown in Fig. 1(b) of the main text.

APPENDIX E: POWER-LAW DECAY AND SUM OF EXPONENTIALS

It is interesting to realize that the choice of a memory kernel, which is a sum of exponentials with different decay rates, can reproduce physical situations where memory decays as a power law, of course with a maximum time cutoff. We are not able to provide a general theory, but visual examples constitute an empirical proof. In Fig. 3 we compare the following three decaying functions of time t:

$$f(x) = t^{-3/2}, \quad \text{(E1)}$$

$$f_3(x) = \sum_{k=1}^{3} \frac{a_k}{\tau_k} e^{-t/\tau_k}, \quad \text{(E2)}$$

$$f_6(x) = \sum_{k=1}^{6} \frac{a_k}{\tau_k} e^{-t/\tau_k}, \quad \text{(E3)}$$

$$\text{with } a_k = \tau_k^{-1/2} \text{ and } \quad \tau \equiv \{1, 10, 100, 0.01, 0.1, 1000\}. \quad \text{(E4)}$$

A more systematic study about how to use exponential functions to approximate power laws is also provided in [46].

[1] A. Cavagna, Phys. Rep. **476**, 51 (2009).
[2] G. Marty and O. Dauchot, Phys. Rev. Lett. **94**, 015701 (2005).
[3] A. Bodrova, A. K. Dubey, S. Puri, and N. Brilliantov, Phys. Rev. Lett. **109**, 178001 (2012).
[4] C. Scalliet, A. Gnoli, A. Puglisi, and A. Vulpiani, Phys. Rev. Lett. **114**, 198001 (2015).
[5] A. Plati and A. Puglisi, Phys. Rev. E **102**, 012908 (2020).
[6] A. Plati, A. Baldassarri, A. Gnoli, G. Gradenigo, and A. Puglisi, Phys. Rev. Lett. **123**, 038002 (2019).
[7] A. Lasanta and A. Puglisi, J. Chem. Phys. **143**, 064511 (2015).
[8] U. Seifert, Annu. Rev. Condens. Matter Phys. **10**, 171 (2019).
[9] A. C. Barato and U. Seifert, Phys. Rev. Lett. **114**, 158101 (2015).
[10] U. Seifert, Physica A **504**, 176 (2018).
[11] T. R. Gingrich, J. M. Horowitz, N. Perunov, and J. L. England, Phys. Rev. Lett. **116**, 120601 (2016).
[12] T. Van Vu and Y. Hasegawa, Phys. Rev. E **100**, 032130 (2019).
[13] Y. Hasegawa and T. Van Vu, Phys. Rev. E **99**, 062126 (2019).
[14] A. Dechant and S.-i. Sasa, Proc. Natl. Acad. Sci. USA **117**, 6430 (2020).
[15] D. Hartich and A. c. v. Godec, Phys. Rev. Lett. **127**, 080601 (2021).
[16] T. J. Doerries, S. A. M. Loos, and S. H. L. Klapp, J. Stat. Mech. (2021) 033202.
[17] T. Franosch, M. Grimm, M. Belushkin, F. M. Mor, G. Foffi, L. Forró, and S. Jeney, Nature (London) **478**, 85 (2011).
[18] F. Zamponi, F. Bonetto, L. F. Cugliandolo, and J. Kurchan, J. Stat. Mech.: Theory Exp. (2005) P09013.
[19] A. Puglisi and D. Villamaina, Europhys. Lett. **88**, 30004 (2009).
[20] A. Crisanti, A. Puglisi, and D. Villamaina, Phys. Rev. E **85**, 061127 (2012).
[21] A. Puglisi, *Transport and Fluctuations in Granular Fluids: From Boltzmann Equation to Hydrodynamics, Diffusion and Motor Effects* (Springer, New York, 2014).
[22] P. Rizkallah, A. Sarracino, O. Bénichou, and P. Illien, Phys. Rev. Lett. **128**, 038001 (2022).
[23] L. P. Fischer, H.-M. Chun, and U. Seifert, Phys. Rev. E **102**, 012120 (2020).
[24] J. S. Lee, J.-M. Park, and H. Park, Phys. Rev. E **104**, L052102 (2021).
[25] A. Dechant, arXiv:2202.10696.
[26] I. Di Terlizzi and M. Baiesi, J. Phys. A: Math. Theor. **53**, 474002 (2020).
[27] A. Sarracino, D. Villamaina, G. Gradenigo, and A. Puglisi, Europhys. Lett. **92**, 34001 (2010).
[28] E. Cortes, B. J. West, and K. Lindenberg, J. Chem. Phys. **82**, 2708 (1985).
[29] T. Munakata and M. Rosinberg, J. Stat. Mech.: Theory Exp. (2013) P06014.
[30] T. Munakata and M. L. Rosinberg, Phys. Rev. Lett. **112**, 180601 (2014).
[31] L. Costanzo, A. Lo Schiavo, A. Sarracino, and M. Vitelli, Entropy **23**, 677 (2021).
[32] L. Costanzo, A. Lo Schiavo, A. Sarracino, and M. Vitelli, Entropy **24**, 1222 (2022).
[33] W. Min, G. Luo, B. J. Cherayil, S. C. Kou, and X. S. Xie, Phys. Rev. Lett. **94**, 198302 (2005).
[34] B. J. Berne, J. P. Boon, and S. A. Rice, J. Chem. Phys. **45**, 1086 (1966).
[35] C. Gardiner, *Stochastic Methods* (Springer-Verlag, Berlin, 2009).
[36] J. L. Lebowitz and H. Spohn, J. Stat. Phys. **95**, 333 (1999).
[37] Note that due to the linearity, the covariances $\hat{\sigma}_{0i}$ do not depend upon F_{ext}.
[38] W. Wanicharpichat, Int. J. Pure App. Math. **108**, 967 (2016).
[39] T. M. Cover, *Elements of Information Theory* (John Wiley & Sons, New York, 1999).
[40] A. Plati and A. Puglisi, Phys. Rev. Lett. **128**, 208001 (2022).
[41] G. Weiss, J. Appl. Probab. **12**, 831 (1975).
[42] D. Lucente, A. Baldassarri, A. Puglisi, A. Vulpiani, and M. Viale, Phys. Rev. Res. **4**, 043103 (2022).
[43] P. Pietzonka, F. Ritort, and U. Seifert, Phys. Rev. E **96**, 012101 (2017).
[44] S. K. Manikandan, D. Gupta, and S. Krishnamurthy, Phys. Rev. Lett. **124**, 120603 (2020).
[45] K. Brandner, K. Saito, and U. Seifert, Phys. Rev. X **5**, 031019 (2015).
[46] T. Bochud and D. Challet, Quant. Finance **7**, 585 (2007).